



PERGAMON

Deep-Sea Research II 48 (2001) 1507–1528

---

---

DEEP-SEA RESEARCH  
PART II

---

---

www.elsevier.com/locate/dsr2

# Interannual variability of oceanic CO<sub>2</sub> and biogeochemical properties in the Western North Atlantic subtropical gyre

Nicholas R. Bates\*

*Bermuda Biological Station For Research, Inc., 17 Biological Station Lane, Ferry Reach, GE01, Bermuda*

---

## Abstract

Understanding the relationship between Earth's climate and the oceanic carbon cycle requires an understanding of the time-variations of CO<sub>2</sub> in the ocean, its exchange with the atmosphere, and the rate of uptake of anthropogenic CO<sub>2</sub> by the ocean. Since 1988, hydrographic and biogeochemical data have been collected at the Bermuda Atlantic Time-Series Study (BATS) site in the Sargasso Sea, located in the North Atlantic subtropical gyre. With over a decade of oceanographic data, interannual trends of CO<sub>2</sub> species and air–sea exchange of CO<sub>2</sub> at BATS can be examined. Between 1988 and 1998, surface seawater total carbon dioxide (TCO<sub>2</sub>) and salinity normalized TCO<sub>2</sub> (*n*TCO<sub>2</sub>) increased at a rate of  $2.2 \pm 6.9$  and  $1.6 \pm 5.8 \mu\text{mol kg}^{-1} \text{yr}^{-1}$ , respectively. During the same period, the partial pressure of CO<sub>2</sub> (*p*CO<sub>2</sub>) of seawater increased at a rate of  $1.4 \pm 10.7 \mu\text{atm yr}^{-1}$ , similar to the rate of increase in atmospheric *p*CO<sub>2</sub> ( $\sim 1.3 \mu\text{atm yr}^{-1}$ ). The increase in seawater TCO<sub>2</sub> and *p*CO<sub>2</sub> can be attributed to a combination of uptake of anthropogenic CO<sub>2</sub> from the atmosphere and interannual changes in hydrographic properties of the subtropical gyre. Underlying interannual trends were examined by determining how hydrographic and biogeochemical anomalies, or deviations from the mean state, vary over time. Significant correlations existed between anomalies of temperature, salinity, integrated primary production, mixed-layer depth, TCO<sub>2</sub>, salinity normalized TCO<sub>2</sub> (*n*TCO<sub>2</sub>), and alkalinity. For example, cold temperature anomalies (up to  $-0.5^\circ\text{C}$ ) in 1992 and 1995 were associated with increased mixed-layer depth, higher rates of integrated primary production ( $< \sim 100 \text{ mg C m}^2 \text{ d}^{-1}$ ), and higher concentrations of *n*TCO<sub>2</sub> ( $< \sim 5 \mu\text{mol kg}^{-1}$ ). The interannual anomalies of hydrography and ocean biogeochemistry were partially linked to large-scale climate variability such as North Atlantic Oscillation (NAO) and El Niño Southern Oscillation (ENSO). Temperature, mixed-layer depth, primary production and TCO<sub>2</sub> anomalies were correlated with NAO variability, with cold anomalies at BATS generally coinciding with NAO negative states. Salinity, alkalinity and *n*TCO<sub>2</sub> anomalies were correlated with the Southern oscillation index (SOI), lagging ENSO events by 6–12 months. © 2001 Published by Elsevier Science Ltd.

---

\* Tel.: + 1-441-236-5022; fax: + 1-441-297-8143.

E-mail address: nick@bbsr.edu (N.R. Bates).

## 1. Introduction

The ocean has an important role in the biogeochemical cycling of carbon and the control of atmospheric CO<sub>2</sub> levels over time. The ocean is estimated to have taken up about 30% of the CO<sub>2</sub> released to the atmosphere through anthropogenic activities during the last few decades. This estimate is based on observations of atmospheric CO<sub>2</sub>, O<sub>2</sub> and δ<sup>13</sup>C records (e.g., Keeling et al., 1989, 1995; Keeling and Shertz, 1992; Francey et al., 1995; Enting et al., 1995), oceanic δ<sup>13</sup>C distributions (Quay et al., 1992), global assessments of the air–sea disequilibrium and gas exchange of CO<sub>2</sub> (e.g., Tans et al., 1990; Takahashi et al., 1997), and ocean models that have been validated with tracers such as bomb radiocarbon (e.g., Sarmiento et al., 1992, 1995; Stocker et al., 1994).

Direct determination of the oceanic accumulation and penetration depth of anthropogenic CO<sub>2</sub> in the ocean can be made using different approaches, including: (1) comparison of preformed preindustrial oceanic total carbon dioxide (TCO<sub>2</sub>) data with contemporary TCO<sub>2</sub> data that has been corrected for changes due to remineralization of organic matter, dissolution of calcium carbonate (e.g., Brewer, 1978; Chen and Millero, 1979; Chen, 1984; Goyet and Brewer, 1993; Goyet et al., 1999) and air–sea disequilibrium (i.e., ΔC\*, Gruber et al., 1996; Gruber, 1998); and (2) oceanic timeseries or repeated surveys of the oceanic CO<sub>2</sub> system which reveal an increase in concentration of CO<sub>2</sub> over time (Wallace, 1995). The first approach has been widely used but is subject to considerable uncertainties (Shiller, 1981; Brewer et al., 1997). Use of the quasi-conservative tracer ΔC\* (Gruber et al., 1996, 1998) or multiparametric analyses (e.g., Goyet et al., 1999) provide the best methods for determining anthropogenic CO<sub>2</sub> inventories in the ocean at present. The second approach is the direct determination of the accumulation of CO<sub>2</sub> over time at time-series sites (e.g., Keeling, 1993; Winn et al., 1994; Bates et al., 1996a; Winn et al., 1998) and repeat measurements of water-column CO<sub>2</sub> properties in selected regions (e.g., Goyet and Peltzer, 1994). This approach is complicated by the fact that small interannual changes of CO<sub>2</sub> can be obscured by larger seasonal variability of CO<sub>2</sub> (e.g., Goyet and Davis, 1997) due to processes, such as seasonal temperature changes, vertical and horizontal mixing, biological production, diurnal warming/cooling, and storm events (Bates et al., 1998d,e), which act on different timescales. Time-series records are further complicated by spatial variability (e.g., mesoscale phenomena), changes in meridional and zonal gradients. Interannual changes in oceanic CO<sub>2</sub> concentrations have been observed at the two US Joint Global Ocean Flux (JGOFS) ocean time-series sites. At the ALOHA site in the North Pacific Ocean, an interannual increase in TCO<sub>2</sub> of ~1 μmol kg<sup>-1</sup> yr<sup>-1</sup> has been observed from 1988 to 1996 and attributed to the uptake of anthropogenic CO<sub>2</sub> from the atmosphere (Winn et al., 1994, 1998). At the Bermuda Atlantic Time-Series Study (BATS) site (32°50'N, 64°10'W; Fig. 1) in the subtropical gyre of the western North Atlantic Ocean, an interannual increase in TCO<sub>2</sub> of ~1.7 μmol kg<sup>-1</sup> yr<sup>-1</sup> between 1988 and 1993 has been observed (Bates et al., 1996a). What remains unclear from the BATS record is how much this increase reflects uptake of anthropogenic CO<sub>2</sub> versus natural variability in the subtropical gyre occurring over interannual timescales.

With a decade of data collected at BATS, interannual trends of ocean biogeochemistry and CO<sub>2</sub> distributions in the Sargasso Sea were examined. This doubles the length of the CO<sub>2</sub> time-series record at BATS first reported by Bates et al. (1996a). Interannual relationships are shown to exist

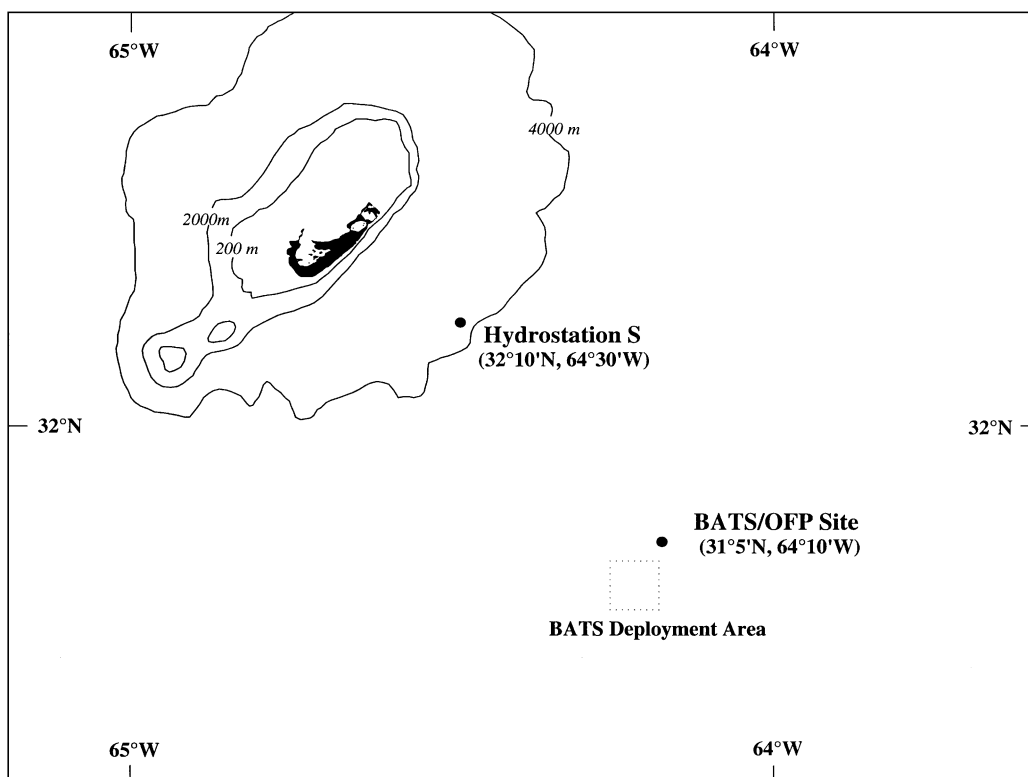


Fig. 1. Location of the BATS site (32°50'N, 64°10'W), Hydrostation S (32°10'N, 64°30'W) and the island of Bermuda.

between CO<sub>2</sub> and hydrographic properties, and indicators of biological activity (e.g., integrated primary productivity). Such patterns provide a broader context for understanding the processes that control the interannual variability of ocean biogeochemistry, CO<sub>2</sub> distributions, and air–sea CO<sub>2</sub> exchange. Part of the physical and biogeochemical variability observed at BATS is driven by natural large-scale climate variability such as the North Atlantic Oscillation (NAO) and El Niño–Southern Oscillation (ENSO). Establishing the underlying links between these larger-scale climate patterns and ocean biogeochemistry will help oceanographers and climate scientists understand anthropogenic changes in the context of natural variability.

## 2. Oceanographic setting

Seasonal variation of ocean biogeochemistry in the Sargasso Sea region of the western North Atlantic subtropical gyre is tightly coupled to variability of wintertime convective mixing. The BATS site is characterized by an 8–10°C seasonal variation in surface temperature and a fluctuation of mixed-layer depth from > 200 m in winter to < 10 m during the summer (Michaels et al., 1994b). During winter, subtropical mode water (STMW; or 18°C mode water) is formed north of

BATS and subsequently subducted within the Sargasso Sea (e.g., Worthington, 1976; Talley and Raymer, 1982; Ebbesmeyer and Lindstrom, 1986; Halliwell et al., 1994). A near isothermal layer of STMW occurs between 300 and 500 m deep at BATS, between the seasonal and permanent thermocline. For most of the year nutrient concentrations remain below detection in the euphotic zone and primary production rates are typically low ( $3\text{--}5\text{ mg C m}^{-3}\text{ d}^{-1}$ ). Winter mixing of nutrients supports a short-lived spring phytoplankton bloom (e.g., Menzel and Ryther, 1960, 1961; Michaels et al., 1994b; Michaels and Knap, 1996) with elevated rates of primary production ( $8\text{--}16\text{ mg C m}^{-3}\text{ d}^{-1}$ ). After the spring bloom the mixed-layer shoals to  $\sim 10\text{--}20\text{ m}$ . Considerable variability of  $\text{CO}_2$  species at different timescales has been observed at BATS (Bates et al., 1996a,b; 1998e); for example, seasonally  $\text{TCO}_2$  varies by  $\sim 40\text{ }\mu\text{mol kg}^{-1}$ , and  $p\text{CO}_2$  varies by  $80\text{--}100\text{ }\mu\text{atm}$ . Seasonal  $\text{TCO}_2$  changes are driven predominantly by biological production, vertical mixing and air–sea gas exchange, while seasonal  $p\text{CO}_2$  variability results primarily from temperature changes.

### 3. Methods

Hydrographic and biogeochemical data has been collected at the BATS site each month since October 1988 using two research vessels, R/V *Weatherbird* and R/V *Weatherbird II*. BATS data are available from several data reports (Knap et al., 1991–1995, 1997a) and at the Bermuda Biological Station For Research (BBSR) web page (<http://www.bbsr.edu>). Water samples and hydrographic data were collected with a SeaBird CTD rosette system and 12-l Niskin samplers. Sampling details have been described previously (Michaels and Knap, 1996; Knap et al., 1997b).  $\text{TCO}_2$  and alkalinity samples were collected into 500-ml Pyrex bottles, poisoned with  $100\text{ }\mu\text{l}$  of saturated  $\text{HgCl}_2$  to prevent biological alteration and sealed with Apiezon grease. A surface seawater supply aboard the R/V *Weatherbird II* has been sampled continuously for temperature, salinity, and seawater  $p\text{CO}_2$  since June 1994 (Bates et al., 1998e).

#### 3.1. $\text{CO}_2$ species measurements

$\text{TCO}_2$  was determined by gas extraction and coulometry (Johnson et al., 1985, 1987). Since 1991, a Single-Operator Multi-Metabolic Analyzer (SOMMA) has been used to determine  $\text{TCO}_2$  (Johnson et al., 1993). Details of  $\text{TCO}_2$  methods are described elsewhere (Bates et al., 1996a,b). Prior to 1991,  $\text{TCO}_2$  was determined by C. Goyet (Woods Hole Oceanographic Institution) using an early version of the SOMMA system. The precision of  $\text{TCO}_2$  analyses was better than 0.025% ( $\sigma = 0.4\text{ }\mu\text{mol kg}^{-1}$ ) based on duplicate and triplicate analyses of  $> 1500$  samples at BBSR from 1991 to 1998. The mean difference between seawater certified reference materials (CRMs; available from A.G. Dickson, Scripps Institution of Oceanography) analyzed at BBSR and their certified value was  $\sim 0.03\%$  ( $\sim 0.5\text{ }\mu\text{mol kg}^{-1}$ ). Analyses of CRMs ensured that the  $\text{TCO}_2$  analyses were highly accurate during the sampling period.

Alkalinity (TA) was determined by potentiometric titration using a modified Gran plot (Gran, 1952; Butler, 1992). Details of alkalinity methods are described elsewhere (Bates et al., 1996a,b). CRM seawater standards were also routinely analyzed for alkalinity. The mean difference between

CRM samples analyzed at BBSR and their certified values was 0.2% ( $\sim 4 \mu\text{mol kg}^{-1}$ ). CRM batches have been assigned alkalinity values by A.G. Dickson (UCSD; <http://www.ucsd.edu>) using a coulometric technique.

Seawater  $p\text{CO}_2$  was determined since June 1994 from a continuously flowing supply of surface seawater using a shower head equilibrator and Licor non-dispersive infrared analyzer. The  $p\text{CO}_2$  system was designed by T. Takahashi and D. Chipman at Lamont Doherty Earth Observatory (LDEO) and detailed methodology is given elsewhere (Bates et al., 1998b–e). Every 30 min, the  $p\text{CO}_2$  system was calibrated with four  $\text{CO}_2$ -in-air standard gases that were previously calibrated against World Meteorological Organization (WMO) standards at LDEO. The precision of the measurement was better than  $1 \mu\text{atm}$  (Bates et al., 1998e). Atmospheric  $p\text{CO}_2$  also was measured from an air supply intake located at about  $\sim 10 \text{ m}$  above sea level on the R/V *Weatherbird II*. The  $p\text{CO}_2$  system measures the mole fraction of  $\text{CO}_2$  ( $x\text{CO}_2$ ) in dry air and atmospheric  $p\text{CO}_2$  data were calculated from atmospheric pressure and water vapor content. Prior to June 1994, seawater  $p\text{CO}_2$  was calculated from  $\text{TCO}_2$  and alkalinity data using those dissociation constants that provided the best comparison to directly measured  $p\text{CO}_2$  (Bates et al., 1996a).

In this paper,  $\text{TCO}_2$  and alkalinity data were “normalized” (i.e.,  $n\text{TCO}_2$  and  $n\text{TA}$ ) to a constant salinity of 36.6, which is the mean salinity at BATS. This removes the effect of local precipitation and evaporation on  $\text{TCO}_2$  and alkalinity. Prior to June 1994, seawater  $p\text{CO}_2$  was calculated from  $\text{TCO}_2$  and alkalinity using dissociation constants that best reproduced directly measured  $p\text{CO}_2$ . As part of our analysis, the atmospheric record of  $x\text{CO}_2$ , determined from flask samples collected from the eastern end of the island of Bermuda by P. Tans and T. Conway (National Center for Atmospheric Research, NCAR; <http://www.cmdl.noaa.gov/>), were compared with shipboard measurements of  $x\text{CO}_2$  and converted to  $p\text{CO}_2$  using surface seawater temperature and salinity values.

### 3.2. Other measurements, data and data analysis

BATS hydrographic data and several biogeochemical parameters are discussed in this paper. Details on the methodologies used are reported elsewhere (e.g., Michaels and Knap, 1996; Knap et al., 1997b; Steinberg et al., 2001). Rates of primary production were determined using  $^{14}\text{C}$  incubation techniques and integrated over the upper water column. Mixed-layer depths were determined using a 0.1 sigma theta change criteria (Sprintall and Tomczak, 1992). Hydrographic data from Hydrostation S ( $32^\circ 10' \text{N}$ ,  $64^\circ 30' \text{W}$ ) in the Sargasso Sea was also used for the period 1954–1998 (<http://www.bsr.edu>). BATS, Hydrostation S data, and climate indices data (e.g., NAO) were compared using cross-correlation analyses (Chatfield, 1989) to determine the statistical validity of biogeochemical and hydrographic relationships. Climate indices for NAO were compiled by the Climate and Global Dynamics (CGD) division at NCAR (<http://www.cgd.ucar.edu/cas/climind/>). Wintertime (December through March) NAO indices were based on sea level pressure (SLP) differences between Lisbon, Portugal and Stykkisholmur, Iceland (Hurrell, 1995). The Southern oscillation index (SOI), an indicator of ENSO state, was compiled by NOAA’s Climate Prediction Center and based on SLP differences between Darwin, Australia and Tahiti, South Pacific Ocean (Trenberth, 1984, 1997; <http://nic.fb4.noaa.gov/dada/cddb>).

## 4. Results and discussion

### 4.1. Hydrographic variability

The BATS site was characterized by a seasonal oscillation in temperature of 7–10°C (Fig. 2a) and variability of salinity ranging from 36.2 to 36.9 (Fig. 2b). Surface and mixed-layer salinity tended to be fresher during the summer and early fall period due to seasonal stratification. Salinity values in the winter and spring of 1997 were particularly elevated compared to other periods of the record.

### 4.2. TCO<sub>2</sub> variability

Surface TCO<sub>2</sub> and salinity normalized TCO<sub>2</sub> (*n*TCO<sub>2</sub>) had a characteristic seasonal variability of ~30–40 μmol kg<sup>-1</sup> (Fig. 2c) which has been observed previously (Bates et al., 1996a). Although TCO<sub>2</sub> variability was inversely related to seasonal temperature changes (Fig. 1a), seasonal variations of TCO<sub>2</sub> appear to reflect seasonal changes in primary production and gas exchange (Bates et al., 1996a, 1998e; Marchal et al., 1996; Gruber et al., 1998).

### 4.3. Alkalinity variability

Surface alkalinity had a variability of ~30 μmol kg<sup>-1</sup> over the duration of the program (Fig. 2d). Upper-ocean alkalinity + nitrate is typically a conservative tracer of salinity (e.g., Brewer and Goldman, 1986; Bates et al., 1998a). In the Sargasso Sea, alkalinity is a function of salinity (note: nitrate concentrations are extremely low and do not impact the proton balance) as previously observed (Bates et al., 1996b). If Sargasso Sea TA data is normalized to the mean salinity of 36.6, salinity normalized alkalinity (*n*TA) showed minor variability about a mean of 2388.4 ± 4.4 μmol kg<sup>-1</sup> (Fig. 2d). If BATS TA data is normalized to a salinity of 35, mean *n*TA values of 2284.0 ± 4.2 μmol kg<sup>-1</sup> are comparable to mean *n*TA values of ~2291 μmol kg<sup>-1</sup> observed elsewhere in the North Atlantic (Millero et al., 1998), with a few notable exceptions. Low *n*TA values observed in February 1992 have been attributed to the effects of calcium carbonate production by either coccolithophores (predominantly *Emiliana huxleyi*) or the foraminifera *Globorotalia truncatoides* (Bates et al., 1996b). Low *n*TA values observed in January 1998 (Fig. 2d) may similarly reflect a rare calcification event.

### 4.4. Seawater and atmospheric pCO<sub>2</sub> variability

Surface seawater pCO<sub>2</sub> and atmospheric pCO<sub>2</sub> have a seasonal variability of ~80–100 and ~20 μatm, respectively (Fig. 3a) as shown previously (Bates et al., 1998e). Seawater pCO<sub>2</sub> variability is closely coupled to temperature variability, reflecting the dominant control of temperature on pCO<sub>2</sub> in the Sargasso Sea (Bates et al., 1998e). The seasonality of atmospheric pCO<sub>2</sub> and xCO<sub>2</sub> (not shown) has a similar magnitude to that observed on the island of Bermuda and other North Atlantic sampling sites (e.g., Key Biscayne, Florida; Terçeira Island, Açores). The Sargasso Sea is a sink for atmospheric CO<sub>2</sub> during winter/spring and a source of CO<sub>2</sub> to the atmosphere during the summer.

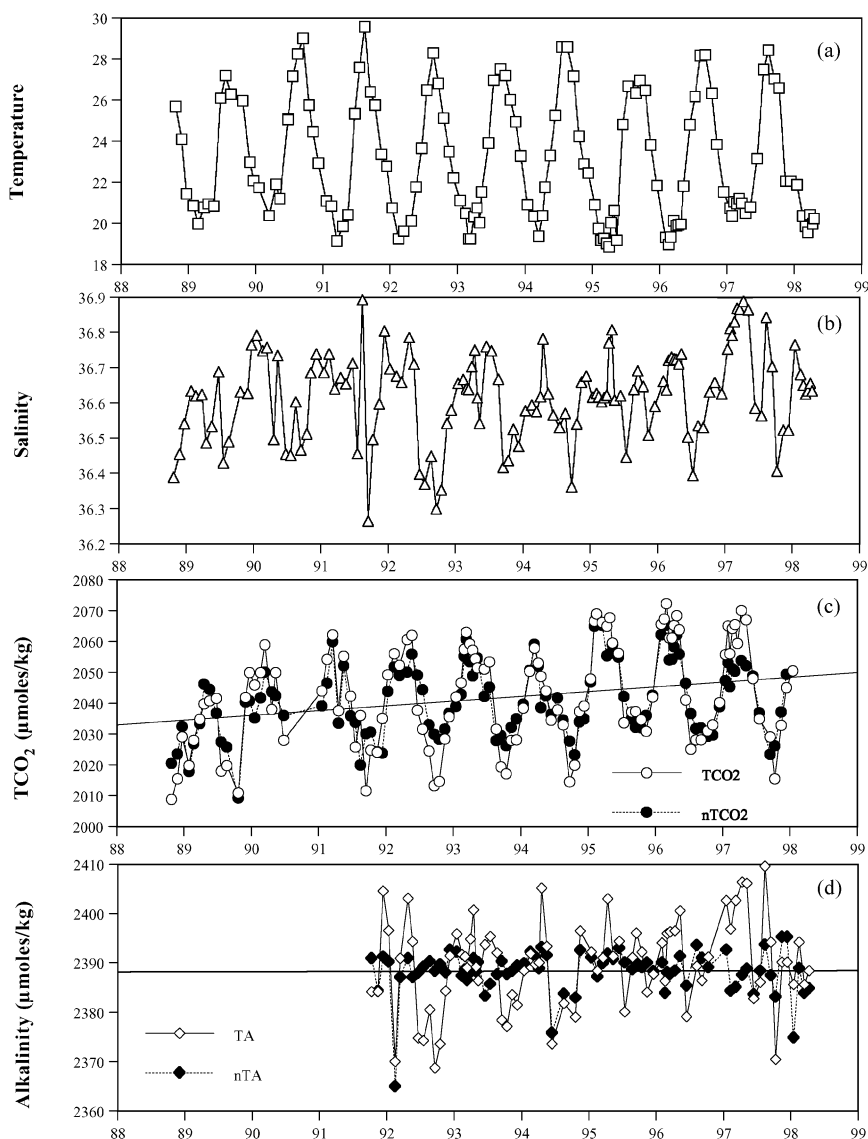


Fig. 2. Time series of surface properties at the BATS site from 1988 to 1998. (a) Temperature ( $^{\circ}\text{C}$ ). (b) Salinity. (c)  $\text{TCO}_2$  (open circles) and salinity normalized  $\text{TCO}_2$  ( $n\text{TCO}_2$ ; closed circles).  $n\text{TCO}_2$  is normalized to a constant salinity of 36.6 (the mean observed salinity at BATS). Units are in  $\mu\text{mol kg}^{-1}$ . The slopes of the regression lines are  $2.04$  ( $\text{TCO}_2$ ) and  $1.55$  ( $n\text{TCO}_2$ )  $\mu\text{mol kg}^{-1} \text{yr}^{-1}$ , respectively. (d) Alkalinity (TA; open diamonds) and salinity normalized alkalinity ( $n\text{TA}$ ; closed diamonds).  $n\text{TA}$  is normalized to a constant salinity of 36.6 (mean observed salinity at BATS). Units are in  $\mu\text{mol kg}^{-1}$ .

#### 4.5. Interannual trends of $\text{CO}_2$ species

There were significant interannual changes in  $\text{TCO}_2$  and  $p\text{CO}_2$  at BATS (Figs. 2 and 3). From 1988 to 1998, surface  $\text{TCO}_2$  increased at a rate of  $2.0 \pm 15.4 \mu\text{mol kg}^{-1} \text{yr}^{-1}$  (or  $\sim 0.1\% \text{yr}^{-1}$ ),

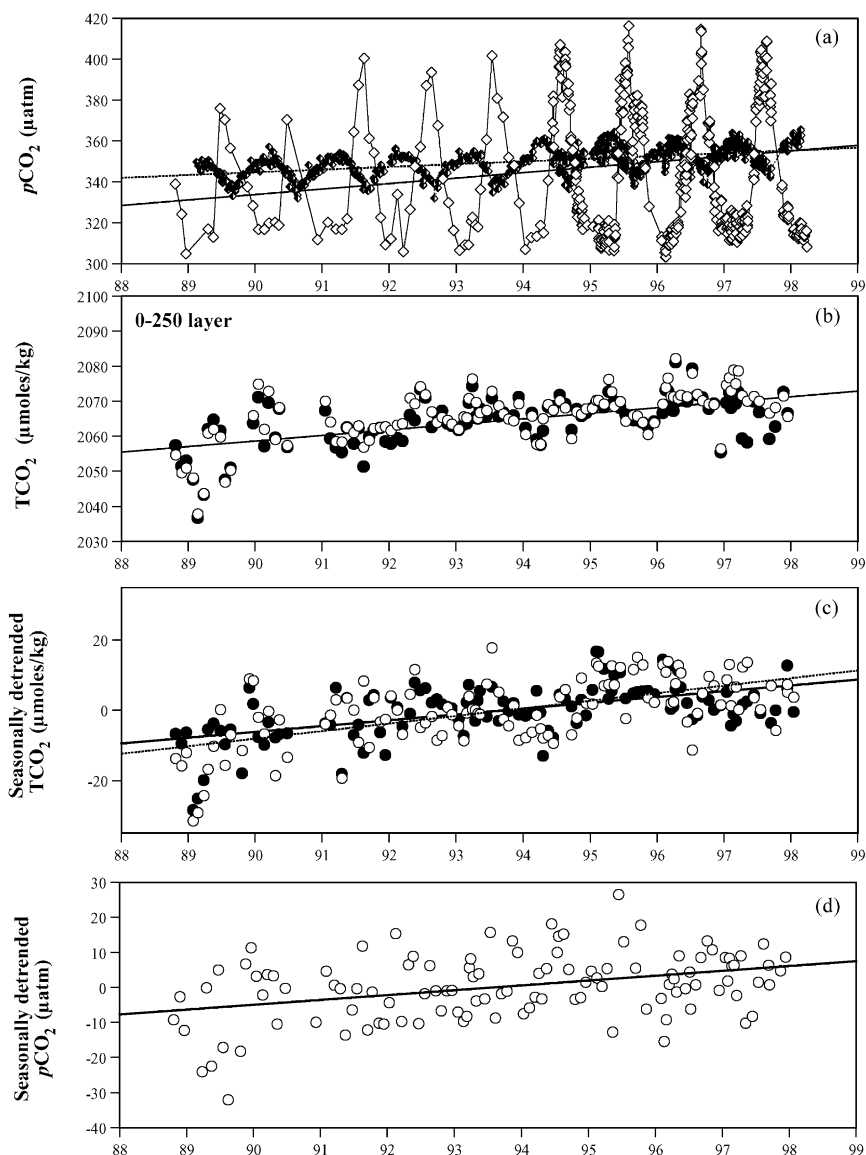


Fig. 3. Time series of water column, surface and atmospheric properties at the BATS site from 1988 to 1998. (a) Surface seawater  $p\text{CO}_2$  ( $\mu\text{atm}$ , open diamond) and atmospheric  $p\text{CO}_2$  ( $\mu\text{atm}$ , closed diamond). The slopes of the regression lines are 2.66 (seawater  $p\text{CO}_2$ ) and 1.33 (atmospheric  $p\text{CO}_2$ )  $\mu\text{atm yr}^{-1}$ , respectively. (b) Mean  $\text{TCO}_2$  (open circles) and salinity normalized  $\text{TCO}_2$  ( $n\text{TCO}_2$ ; closed circles) in the 0–250 m layer. The slopes of the regression lines are 1.85 ( $\text{TCO}_2$ ) and 1.59 ( $n\text{TCO}_2$ )  $\mu\text{mol kg}^{-1} \text{yr}^{-1}$ , respectively. (c) Seasonally detrended  $\text{TCO}_2$  (open circles) and  $n\text{TCO}_2$  (closed circles) in the surface layer. The slopes of the regression lines are 2.2 ( $\text{TCO}_2$ ) and 1.6 ( $n\text{TCO}_2$ )  $\mu\text{mol kg}^{-1} \text{yr}^{-1}$ , respectively. (d) Seasonally detrended  $p\text{CO}_2$  (open circles) in the surface layer. The slope of the regression lines is 1.4  $\mu\text{atm yr}^{-1}$ .

similar to the rate of increase (i.e., 1.7  $\mu\text{mol kg}^{-1} \text{yr}^{-1}$ ) in  $\text{TCO}_2$  previously reported by Bates et al. (1996a) from 1988 to 1993. Since 1988, surface  $\text{TCO}_2$  has increased by almost 20  $\mu\text{mol kg}^{-1}$  (Fig. 2c). A slightly smaller increase of  $1.6 \pm 11.5 \mu\text{mol kg}^{-1} \text{yr}^{-1}$  (0.08% change per year) was

Table 1

Rates of increase of seawater  $\text{TCO}_2$ ,  $n\text{TCO}_2$  and  $p\text{CO}_2$  at the BATS site (1988–1998)

	Rate of increase at BATS (1988–1998)
$\text{TCO}_2$	$2.2 \pm 6.9 \mu\text{mol kg}^{-1} \text{yr}^{-1}$
$n\text{TCO}_2$	$1.6 \pm 5.8 \mu\text{mol kg}^{-1} \text{yr}^{-1}$
$p\text{CO}_2$	$1.4 \pm 10.7 \mu\text{atm yr}^{-1}$

observed for salinity-normalized  $\text{TCO}_2$  ( $n\text{TCO}_2$ ). Similar rates of increase were observed in the 0–250 m layer (Fig. 3b) and in the subtropical mode water (not shown; Bates et al., 1996a). The error estimates for these rates of  $\text{TCO}_2$  increase were large because of the seasonal variability of  $\text{TCO}_2$ . A more useful method involves removing the seasonal variability and evaluating rates of increase using seasonally detrended data. Rates of increase of  $\text{TCO}_2$  and  $n\text{TCO}_2$  were  $2.2 \pm 6.9$  and  $1.6 \pm 5.8 \mu\text{mol kg}^{-1} \text{yr}^{-1}$ , respectively, for seasonally detrended data (Fig. 3c; Table 1).

From 1988 to 1998, atmospheric  $x\text{CO}_2$  (mole fraction of  $\text{CO}_2$  in dry air), measured at the Bermuda East atmospheric sampling site on the island of Bermuda (P. Tans and T. Conway, NCAR), increased at a rate of  $1.3 \mu\text{atm yr}^{-1}$  (Fig. 3a). The increase in atmospheric  $\text{CO}_2$  concentrations was similar to that observed at other atmospheric  $\text{CO}_2$  sampling sites across the subtropical latitudes. The increase in seawater  $p\text{CO}_2$  at BATS from 1988 to 1998 was  $1.4 \pm 18.8 \mu\text{atm yr}^{-1}$ . The large error estimate ( $\pm 18.8 \mu\text{atm}$ ) reflects the seasonal variability of seawater  $p\text{CO}_2$  ( $\sim 80$ – $100 \mu\text{atm}$ ), which makes determining the rate of increase difficult over the 10-yr sampling period. If seasonally detrended (i.e., seasonal variability removed) data is used, seawater  $p\text{CO}_2$  increased at a rate of  $1.4 \pm 10.7 \mu\text{atm yr}^{-1}$  (Fig. 3d). Thus the rates of seawater and atmospheric  $p\text{CO}_2$  increases were similar in magnitude.

The  $1.6 \mu\text{mol kg}^{-1} \text{yr}^{-1}$  increase of  $n\text{TCO}_2$  (given the temperature, salinity,  $\text{TCO}_2$  and TA properties of the Sargasso Sea) should theoretically manifest itself as a  $2.6 \mu\text{atm yr}^{-1}$  increase in seawater  $p\text{CO}_2$ , a rate double the observed increase. What are the causes for the differences between the observed ( $1.4 \pm 10.7 \mu\text{atm yr}^{-1}$ ) and theoretical ( $2.6 \mu\text{atm yr}^{-1}$ ) rates of increase? It may be that the sampling period is not long enough to adequately resolve a rate of  $p\text{CO}_2$  increase given the errors ( $\pm 10.7 \mu\text{atm}$ ) associated with seasonally detrended data (Fig. 3d). Another factor is that the rate of increase is complicated by interannual variability of hydrographic properties in the Sargasso Sea. Between 1988 and 1998, mean surface salinity has increased by 0.11 salinity units. This change has manifested itself as an increase in  $\text{TCO}_2$  of  $\sim 6 \mu\text{mol kg}^{-1}$  over 10 years (compare difference between the rate of increase of  $\text{TCO}_2$ ,  $2.2 \mu\text{mol kg}^{-1} \text{yr}^{-1}$ , and  $n\text{TCO}_2$ ,  $1.6 \mu\text{mol kg}^{-1} \text{yr}^{-1}$ ). Alkalinity also has increased by  $\sim 8 \mu\text{mol kg}^{-1}$  between 1988 and 1998 ( $0.8 \pm 11.5 \mu\text{mol kg}^{-1} \text{yr}^{-1}$ ). Seawater  $p\text{CO}_2$  theoretically should increase at a rate of  $1.3$ – $1.7 \mu\text{atm yr}^{-1}$  (the range in rates reflects the range of water temperatures at BATS), given that there was a  $1.6 \mu\text{mol kg}^{-1} \text{yr}^{-1}$  increase of  $n\text{TCO}_2$  and  $0.8 \mu\text{mol kg}^{-1} \text{yr}^{-1}$  increase in TA. This theoretical rate ( $1.3$ – $1.7 \mu\text{atm yr}^{-1}$ ) is similar to observed rate of seawater  $p\text{CO}_2$  increase (i.e.,  $1.4 \mu\text{atm yr}^{-1}$ ). Establishing the underlying interannual trends reveals that oceanic  $\text{CO}_2$  concentrations in the North Atlantic subtropical gyre are increasing at a rate similar to the atmosphere. A similar finding has been shown occurring at the ALOHA site in the North Pacific subtropical gyre (Winn et al., 1994, 1998).

#### 4.6. Interannual relationships of temperature, primary production and $\text{TCO}_2$

BATS data provide a useful window on interannual variability in the Sargasso Sea. One approach to investigating interannual changes is to compare hydrographic and biogeochemical anomalies over time. In Figs. 4 and 5, anomalies of temperature, salinity,  $\text{TCO}_2$ , alkalinity, mixed-layer depths and primary production were compared to reveal underlying connections that help explain the causes of interannual variability. In the method, a composite year of data is compiled for each parameter from the entire 1988–1998 data set. We use a polynomial fit of the data to predict the positive or negative deviations of a parameter from this ideal fit for the entire time-series record. A six-month running mean is then applied to the monthly anomalies. For example, a plot of temperature anomaly (Fig. 4a) indicates periods when the surface layer was warmer (warm or positive anomaly) or cooler (cold or negative anomaly) than the mean. Anomalies of other parameters (e.g., salinity,  $\text{TCO}_2$ , alkalinity, integrated primary production) show periods when each parameter was higher or lower than the mean. Similar approaches, for example, have been used to examine the relationships between interannual variability of thermo-

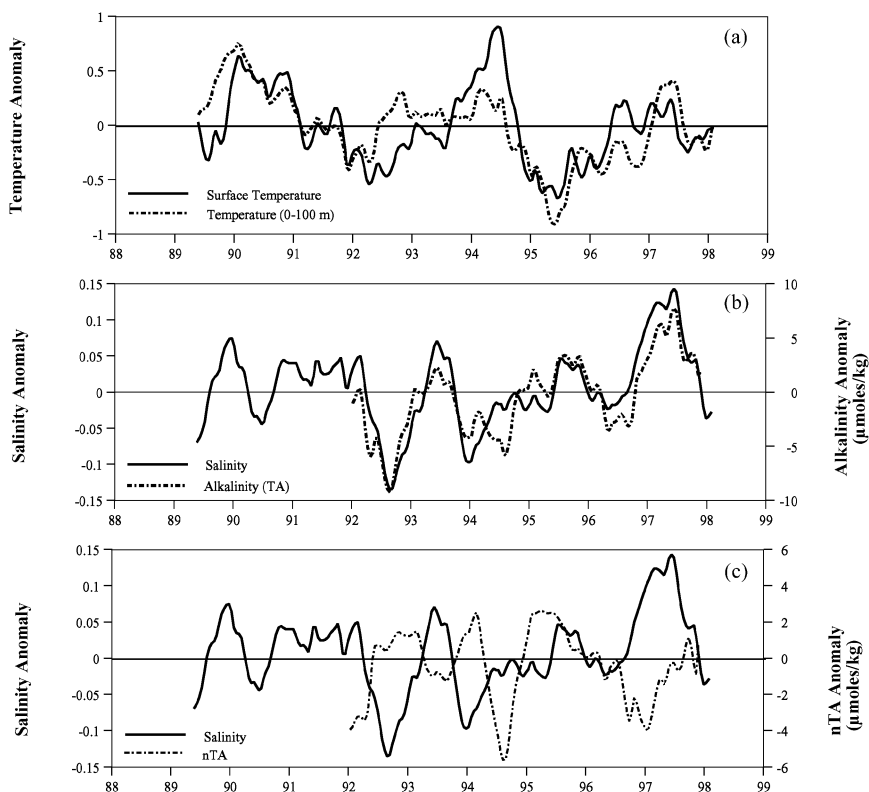


Fig. 4. Time-series of temperature, salinity and alkalinity anomalies at BATS from 1988 to 1998. The plotted anomalies are 6 month running mean through bimonthly and monthly data. (a) Surface temperature (solid line) and mean temperature in the upper 100 m (dashed line). (b) Surface salinity (solid line) and alkalinity (TA) (dashed line). (c) Surface salinity (solid line) and salinity normalized alkalinity ( $n\text{TA}$ ) (dashed line).

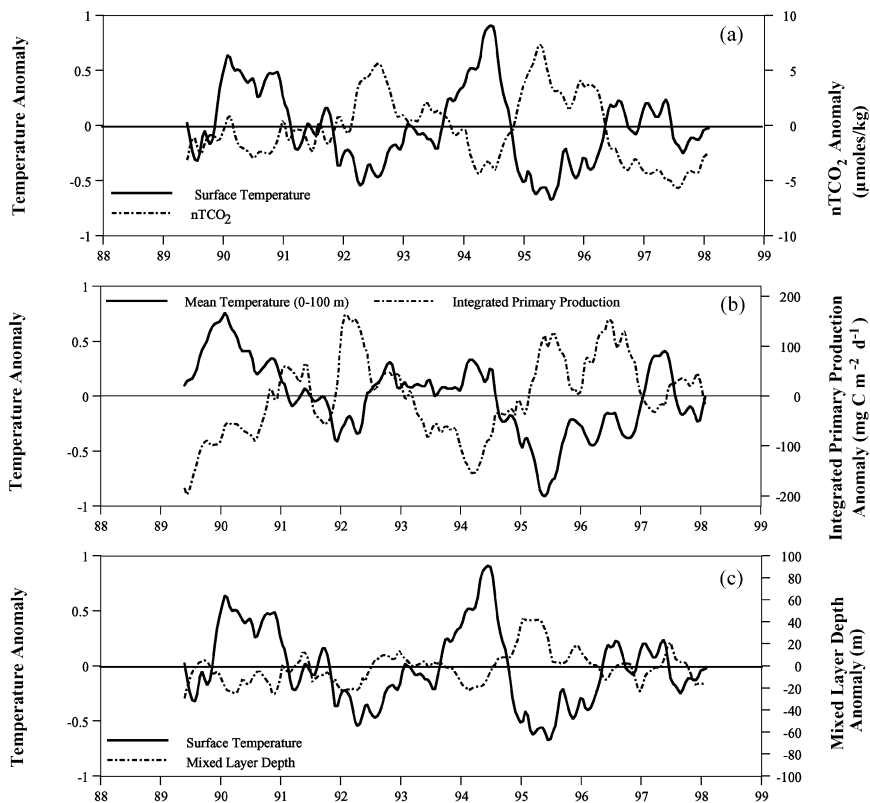


Fig. 5. Time-series of temperature,  $\text{TCO}_2$ , primary production and mixed-layer depth anomalies at BATS from 1988 to 1998. The plotted anomalies are 6 month running mean through bimonthly and monthly data. (a) Surface temperature (solid line) and  $n\text{TCO}_2$  (dashed line).  $n\text{TCO}_2$  data are corrected for an interannual increase of  $1.6 \mu\text{mol kg}^{-1} \text{yr}^{-1}$ . (b) Mean temperature in the 0–100 m layer (solid line) and integrated primary production (dashed line). (c) Mean temperature in the surface layer (solid line) and mixed-layer depth (dashed line). Positive mixed-layer anomaly indicates deeper mixed-layer depth.

haline properties in the Sargasso Sea and modes of climate variability (e.g., NAO changes) in the North Atlantic Ocean (e.g., Curry et al., 1998; Joyce and Robbins, 1996).

Two different types of interannual variability were observed in the BATS data: (1) inverse relationships between salinity, alkalinity and salinity normalized alkalinity ( $n\text{TA}$ ), which appear to reflect changes in the water masses observed at BATS; and (2) inverse relationships between temperature,  $n\text{TCO}_2$  and integrated primary production, which appear to be related to climate variability associated with ENSO and NAO phenomenology (see Section 4.8).

The salinity anomaly is compared to TA (Fig. 4b) and the salinity normalized alkalinity ( $n\text{TA}$ ) anomaly (Fig. 4c). The salinity anomaly is characterized by alternating saline and fresh anomalies and the most extreme positive salinity anomaly ( $\sim 0.15$  salinity units) was observed in 1997. Alkalinity anomaly was correlated with the salinity anomalies (Fig. 4b), this relationship having a cross-correlation coefficient of 0.69 (Table 2). Salinity normalized alkalinity ( $n\text{TA}$ ), however, was inversely correlated with salinity (coefficient of  $-0.37$ ; Table 1), indicating that  $n\text{TA}$  was less when more saline water is present at BATS. This observation appears to be consistent with meridional

Table 2

Correlation coefficients for hydrographic and biogeochemical anomalies at BATS (1988–1998), and modes of climate variability (i.e., Southern oscillation index, SOI; North Atlantic oscillation, NAO). Coefficients less than 0.2 are not reported

	SOI <sup>b</sup>	NAO	SST	Temp. (0–100 m)	Salinity	TCO <sub>2</sub>	<i>n</i> TCO <sub>2</sub>	TA	<i>n</i> TA	ML	PP
SO index <sup>a,b</sup>	—	—	—	—	—	—	—	—	—	—	—
NAO index <sup>a</sup>	–0.43	—	—	—	—	—	—	—	—	—	—
Surface temperature (SST) <sup>a</sup>	0.28 <sup>b</sup>	0.40	—	—	—	—	—	—	—	—	—
Temperature (0–100 m) <sup>a</sup>	0.35 <sup>b</sup>	0.42	–0.66	—	—	—	—	—	—	—	—
Salinity <sup>a</sup>	0.52 <sup>b</sup>	–0.48	—	—	—	—	—	—	—	—	—
TCO <sub>2</sub> <sup>a</sup>	—	–0.46	–0.54	–0.38	0.44	—	—	—	—	—	—
NTCO <sub>2</sub> <sup>a</sup>	–0.53 <sup>b</sup>	—	–0.65	–0.45	–0.39	0.64	—	—	—	—	—
Alkalinity (TA) <sup>a</sup>	0.34	–0.52	—	—	0.69	0.25	—	—	—	—	—
NTA <sup>a</sup>	–0.41	—	—	—	–0.37	–0.39	0.38	—	—	—	—
Mixed layer (ML) <sup>a</sup>	0.35 <sup>b</sup>	–0.32	–0.56	–0.45	—	0.40	0.49	—	—	—	—
Primary production (PP) <sup>a</sup>	–0.21 <sup>b</sup>	–0.33	–0.51	–0.64	—	0.35	0.32	—	—	0.20	—

<sup>a</sup>6-month running mean of anomaly.

<sup>b</sup>A lag of 6 months to the SO index gives the best correlations between SOI, hydrographic and biogeochemical parameters.

gradients of alkalinity in the subtropical gyre. Salinity normalized alkalinity tends to increase northwards in the subtropical gyre (Bates et al., 1996c; Millero et al., 1998) as climatological salinity decreases northwards. This northward meridional gradient reflects the increased contribution of upwelled subsurface water that has higher *n*TA due to dissolution of calcium carbonate at depth. Hence, in the northern parts of the Sargasso Sea, there appears to be higher alkalinity per unit salinity. Towards the south, there is less alkalinity per unit salinity. The inverse relationship between salinity and *n*TA anomalies observed at BATS appears to reflect changes between waters with more “northern” subtropical gyre characteristics (i.e., lower salinity, higher *n*TA) and “southern” subtropical gyre characteristics (i.e., higher salinity, lower *n*TA).

Relationships were observed between temperature anomalies, salinity normalized TCO<sub>2</sub> (*n*TCO<sub>2</sub> anomalies were corrected to account for an interannual rate of increase of 1.6 μmol kg<sup>–1</sup> yr<sup>–1</sup>) and integrated primary production anomalies (Fig. 5a and b). For example, three warm anomalies (from 1989 to mid-1991; 1994; early 1997) and two cold anomalies (from mid-1991 to 1993; 1995–1996) were observed from 1988 to 1998 (Fig. 5a). During the warm anomaly periods, surface temperature was up to 0.5°C warmer than the mean temperature for that time of year. Surface temperature anomalies were inversely correlated with both surface TCO<sub>2</sub> (coefficient of –0.54, Table 2) and *n*TCO<sub>2</sub> (coefficient of –0.65). Thus, surface TCO<sub>2</sub> (i.e., corrected *n*TCO<sub>2</sub>) was lower during warm anomalies and higher during cold anomalies (Fig. 5a).

The range of  $\text{TCO}_2$  variability was about  $10 \mu\text{mol kg}^{-1}$ , about one-third of the observed seasonal variability at BATS. Rates of integrated primary production also were inversely correlated with temperature (coefficient of  $-0.64$ , Table 2; Fig. 5b). Since integrated primary production rates sum the biological activity in the upper 100 m or so, we have compared primary production anomalies to temperature anomalies in the upper 100 m. During warm anomalies, rates of integrated primary production were lower by up to  $200 \text{ mg C m}^{-2} \text{ d}^{-1}$  (significant compared to annual ranges of integrated primary production of  $\sim 200\text{--}1400 \text{ mg C m}^{-2} \text{ d}^{-1}$ ). During cold anomalies, rates of integrated primary production were higher. For example, the cold anomaly that spans 1995 and 1996 coincides with higher rates of integrated primary production, increased mixed-layer depth and elevated  $n\text{TCO}_2$ .

Clearly, positive and negative anomalies of integrated primary production and  $n\text{TCO}_2$  were in phase with each other throughout the BATS program. What are the potential causes for the inverse relationships between temperature and integrated primary productivity and  $n\text{TCO}_2$ ? There are several causes that may be linked, including: (1) changes in vertical mixing; and (2) changes in water mass characteristics, circulation of the subtropical gyre and distribution of mesoscale eddies. Variability of vertical mixing could be a potential cause of the observed relationships. For example, during cold-anomaly periods, rates of primary production and  $n\text{TCO}_2$  concentrations were elevated, while mixed layers were typically deeper (Fig. 5c). Mixed-layer depth was inversely correlated with surface temperature (coefficient of  $-0.56$ , Table 2). Michaels and Knap (1996) have shown at the BATS site that in years with deep, cold mixed layers, winter mixed-layer nitrate concentrations and rates of new production were elevated when compared to years with shallow, warmer mixed layers. They also show that winter nitrate concentrations in the upper 500 m at BATS increase with decreasing temperature (Michaels and Knap, 1996, their Fig. 14). Thus deeper vertical mixing and enhanced upward nitrate fluxes during cold anomalies may adequately explain elevated rates of primary production. One problem with this scenario is explaining why  $n\text{TCO}_2$  concentrations were elevated during cold anomalies. Deeper vertical mixing should bring upwards subsurface  $\text{CO}_2$  since  $\text{TCO}_2$  increases vertically with depth (Bates et al., 1996a), but this additional  $\text{CO}_2$  should be subsequently removed through photosynthetic fixation. An explanation for the  $n\text{TCO}_2$  anomaly patterns relates to the non-Redfield entrainment of  $\text{TCO}_2$  and nutrients into the euphotic zone from deeper waters through vertical mixing. The “carbocline”, a rapid increase in  $\text{TCO}_2$  at depth (which is analogous to the nitracline), occurs at much shallower depths ( $\sim 30\text{--}50 \text{ m}$ ) than the nitracline ( $\sim 100\text{--}120 \text{ m}$ ) in the Sargasso Sea. Thus vertical mixing will tend to bring higher than Redfield proportions of  $\text{TCO}_2$  into the mixed layer leaving residual  $n\text{TCO}_2$  anomalies that cannot be removed through new production. Another problem with the vertical mixing scenario is explaining how changes in vertical mixing could elevate rates of primary production and  $n\text{TCO}_2$  concentrations during summer periods of stratification and shallow mixed layers ( $\sim 5\text{--}30 \text{ m}$ ). Since mixed-layer depths were deeper during summer cold anomalies, elevated  $n\text{TCO}_2$  should result from mixing into the shallow “carbocline”. It is not clear why rates of primary production should be elevated during these periods.

A second, perhaps linked scenario, might involve changes in subtropical gyre circulation, distribution of mesoscale eddies and sources of water present at BATS. Mean meridional gradients measured at the longitude of BATS ( $\sim 64^\circ \text{W}$ ) indicate that  $n\text{TCO}_2$  increases northwards towards the site of  $18^\circ \text{C}$  mode water formation and  $n\text{TCO}_2$  decreases southwards into the more permanently stratified Sargasso Sea (Bates et al., 1996c). It should be noted that there is large spatial

variability in the data due to the influence of eddy features. In a general sense, any changes in water masses between those with more “northern” (i.e., cooler, elevated  $n\text{TCO}_2$  and higher primary production) or “southern” (i.e., warmer, reduced  $n\text{TCO}_2$  and lower primary production) characteristics might replicate the observed anomalies of temperature, primary production and  $n\text{TCO}_2$ . Such alternation of water masses might result from oscillation in the position of the subtropical frontal zone that separates areas dominated by easterly or westerly wind patterns in the Sargasso Sea between  $25^\circ\text{N}$  and  $32^\circ\text{N}$  (Halliwell et al., 1994).

Siegel et al. (1999), in their analysis of mean climatological dynamic anomaly fields and associated geostrophic circulation, show a very weak mean westward flow ( $0.5\text{ cm s}^{-1}$ ) near BATS and a stronger east–northeastward flow (up to  $11\text{ cm s}^{-1}$ ) to the north–northwest of the BATS site (their Plate 3). The BATS site falls within a region (oriented in a ESE–WNW direction) where there is near zero mean geostrophic circulation. The BATS site is therefore in a transition zone between easterlies and westerlies and should be influenced by internannual changes in atmospheric and oceanic forcing (see Section 4.8).

Mesoscale eddies have long been thought to influence upper ocean biogeochemistry in the Sargasso Sea (e.g., McGillicuddy and Robinson, 1997; McGillicuddy et al., 1999), and they also may contribute to the interannual variability at BATS. Analysis of sea level anomaly (SLA) fields reveal mesoscale features propagating westward throughout the Sargasso Sea (Siegel et al., 1999; [http://www.icess.ucsb.edu/~davey/TP\\_BATS/BATS\\_sla\\_currents.mpg](http://www.icess.ucsb.edu/~davey/TP_BATS/BATS_sla_currents.mpg)). Notably, SLA variability and eddy kinetic energy (EKE) increases northwards of the BATS site (Siegel et al., 1999, their Plate 3). Recent field studies have indicated that some cyclonic mesoscale eddies manifest themselves at the surface, having cooler *surface* temperatures, higher *surface*  $n\text{TCO}_2$  concentrations, and higher phytoplankton biomass within the euphotic zone compared to surrounding waters and anticyclonic features (McGillicuddy and Robinson, 1997; McGillicuddy et al., 1998; N. Bates, D. McGillicuddy, unpublished data, 1998). If the dynamics of gyre circulation change and the frequency of cyclonic eddies (which have a near surface expression) passing in the vicinity of BATS increases, this also might partially explain periods of cooler anomalies and positive  $n\text{TCO}_2$  and primary production anomalies. A detailed evaluation of this scenario is beyond the scope of this contribution.

#### 4.7. $\text{CO}_2$ anomalies and air–sea $\text{CO}_2$ exchange

Interannual changes of temperature and  $n\text{TCO}_2$  anomalies have minimal effect on rates of air–sea exchange of  $\text{CO}_2$ . For example, during the warm anomaly period in 1994, the surface temperature anomaly of  $\sim 0.5^\circ\text{C}$  (Fig. 5a) acts to increase seawater  $p\text{CO}_2$  by about  $7\text{--}8\ \mu\text{atm}$ . This change in seawater  $p\text{CO}_2$  results from the thermodynamic effect of temperature on  $p\text{CO}_2$  at a rate of 4.23% change in  $p\text{CO}_2$  per  $1^\circ\text{C}$  change in temperature (e.g., Takahashi et al., 1993). At the same time in 1994, lower than normal  $n\text{TCO}_2$  of  $\sim 5\text{--}6\ \mu\text{mol kg}^{-1}$  (Fig. 5a) acts to reduce  $p\text{CO}_2$  by about  $7\text{--}8\ \mu\text{atm}$ . Thus temperature and  $n\text{TCO}_2$  anomalies act upon seawater  $p\text{CO}_2$  in opposite directions effectively cancelling each other.

#### 4.8. Potential connections to modes of climate variability (e.g., ENSO and NAO)

Is there any relationship between these biogeochemical patterns observed in the Sargasso Sea and modes of climate variability such as NAO and ENSO? It is evident from the BATS data that

there was interannual variability in vertical mixing and biogeochemistry and, that this variability is linked to changes in atmospheric forcing. The dominant mode of atmospheric variability in the North Atlantic region is the NAO, which is a dipole meridional oscillation in atmospheric pressure between the Iceland Low and Açores High (Hurrell, 1995; Hurrell and Van Loon, 1997). Strong eastward air flow between the Iceland Low and Açores High carries storms towards western Europe from North America. If the NAO index is negative, storm tracks are thought to shift southward, cooling surface waters, enhancing 18°C mode water formation and deepening winter mixed layers (Rodwell et al., 1999). During positive NAO winters, westerlies that usually prevail in the region between Florida and Cape Hatteras (west of the Açores High) weaken. Reduced wind stress and heat exchange lead to the development of warm temperature anomalies in the subtropical gyre (Bjerknes, 1964; Cayan, 1992a, b) with a magnitude between 0.2 to 0.4°C (Davies et al., 1997; Kapala et al., 1998). Although the NAO is the dominant mode of mid-latitude atmospheric variation, dynamical relations between El Niño and Atlantic climate have long been documented (e.g., Enfield and Mayer, 1997; see references in Penland and Matrosova, 1998). For example, the Gulf Stream position shifts northwards after El Niño events and during NAO positive phases with a lag of  $\sim 2$  yr (Taylor et al., 1998; Taylor and Stephens, 1998). Within 4–12 months of El Niño warming in the Pacific Ocean, warming is observed in the tropical North Atlantic, Caribbean Sea and the SE subtropical gyre (e.g., Zhang et al., 1996; Bojariu, 1997; Penland and Matrosova, 1998). The mechanism for this apparently relates to a reduction in cloud cover in the drier, more stable Atlantic atmosphere (e.g., Zhang et al., 1996; Davies et al., 1997; Jones and Thorncroft, 1998).

Previous studies have related variability in 18°C mode water formation to NAO. Dickson et al. (1996) suggested that the formation of 18°C mode water was enhanced during winters with negative NAO phases when storms track further south and there were more frequent outbreaks of cold air from North America crossing the Sargasso Sea. Other studies have unsuccessfully related mode water variability to atmospheric forcing (e.g., Talley and Raymer, 1982). Jenkins (1982) proposed a storage mechanism by which the cumulative effect of successive winters force changes in mode water (Hazeleger and Drifjhout, 1998), making correlations to modes of climate variability difficult to demonstrate.

Correlations were evident between NAO and hydrographic and biogeochemical properties of the upper ocean (shallower than 18°C mode water) at BATS. Temperature anomalies at BATS were positively correlated with NAO (Table 2; Figs. 6a, 7a), supporting the assertion that the subtropical gyre warms during NAO positive phases (Bjerknes, 1964; Cayan, 1992a, b; Davies et al., 1997; Kapala et al., 1998). NAO negatively correlated with anomalies of salinity, TCO<sub>2</sub>, alkalinity, mixed-layer depth and primary production anomalies at BATS (Table 2). A correlation between temperature and NAO was also evident in the longer Hydrostation S record (1954–1998; Table 3). The coefficients of variability range from 0.32 to 0.52 (Table 2), which is surprisingly high given the inherent spatial variability and mesoscale phenomena at the BATS site (e.g., McGillicuddy et al., 1999; Siegel et al., 1999) and the inherent variability of the atmospheric data. These analyses indicate that the observed inverse relationships between temperature and biogeochemical properties in the Sargasso Sea were linked to NAO variability.

Correlations between the Southern oscillation index (SOI) (i.e., an indicator of ENSO variability) and BATS data were less evident. The best correlations were obtained when a 6-month lag was applied to SO index data. ENSO phases correlated with negative salinity, alkalinity, *n*TCO<sub>2</sub>, temperature and mixed-layer depth anomalies (Table 2; Figs. 6b and 7b). A similar correlation

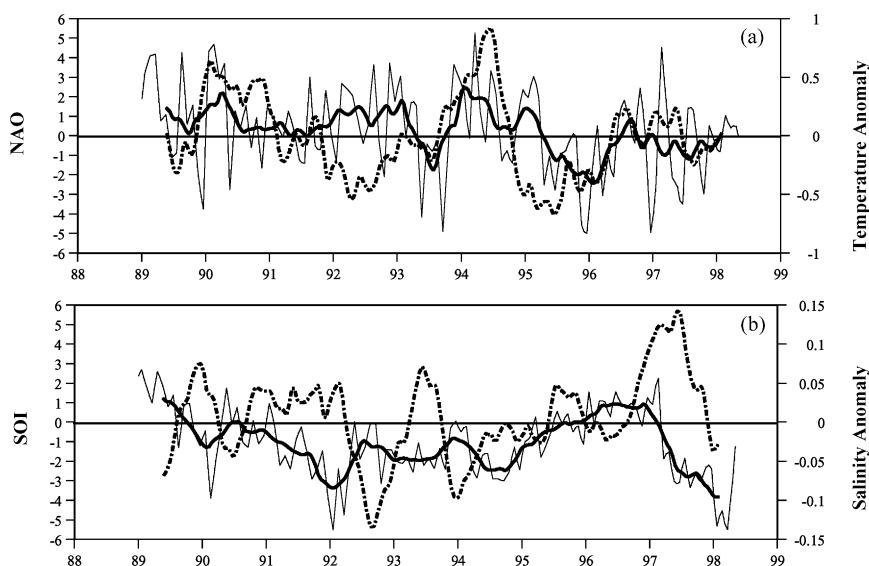


Fig. 6. Time-series of hydrographic anomalies at BATS and modes of climate (1988–1998). 6 month running means are plotted. (a) Temperature anomaly (dashed line) and NAO (solid line). (b) Salinity anomaly (dashed line) and SO index (solid line).

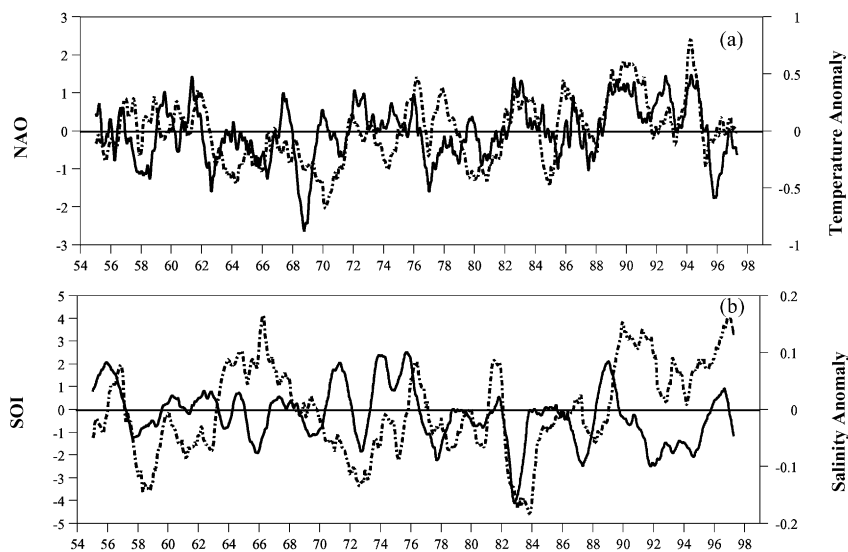


Fig. 7. Time-series of hydrographic anomalies at Hydrostation S and modes of climate variability (1954–1998). 12 month running means are plotted. (a) Temperature anomaly (dashed line) and NAO (solid line). (b) Salinity anomaly (dashed line) and SO index (solid line).

between SO index and salinity was observed in the Hydrostation S data between 1977 and 1998 (Table 3). A poor correlation is evident for the entire 1954–1998 Hydrostation S record, but it should be remember that entrainment of “Great Salinity Anomaly” waters (Dickson et al., 1988) into the upper waters of the subtropical gyre during the 1960s and 1970s affected the salinity

Table 3

Correlation coefficients for hydrographic and biogeochemical anomalies at Hydrostation S, and modes of climate variability (i.e., Southern oscillation index, SOI; North Atlantic oscillation, NAO). Coefficients less than 0.2 are not reported

	SOI <sup>b</sup>	NAO	SST	Salinity
Hydrostation S (1954–1998)				
SO index <sup>a,b</sup>	—	—	—	—
NAO index <sup>a</sup>	—	—	—	—
Surface temperature (SST) <sup>a</sup>	—	0.42	—	—
Salinity <sup>a</sup>	—	—	—	—
Hydrostation S (1977–1998)				
SOI index <sup>a,b</sup>	—	—	—	—
NAO index <sup>a</sup>	—	—	—	—
Surface temperature (SST) <sup>a</sup>	—	0.57	—	—
Salinity <sup>a</sup>	0.37 <sup>b</sup>	—	—	—

<sup>a</sup>12-month running mean of anomaly, SO and NAO index.

<sup>b</sup>A lag of 6 months to the SO index gives the best correlations between SO and salinity anomaly.

budget of the Sargasso Sea. During El Niño phases, freshening of the mixed layer at BATS coincides with a record of increased precipitation on the island of Bermuda (R. Williams, Bermuda Weather Service; National Climatic Data Center (NCDC) data from Bermuda). The 6-month lag of El Niño in the Sargasso Sea compares to a similar lag observed in the tropical North Atlantic and Caribbean Sea in other climatological studies (e.g., Zhang et al., 1996; Bojariu, 1997; Penland and Matrosova, 1998).

The inverse correlation between the SO index and salinity normalized  $\text{TCO}_2$  ( $n\text{TCO}_2$ ) and alkalinity ( $n\text{TA}$ ) also hints at changes in circulation patterns discussed earlier (Section 4.6). On previous BATS spatial “validation” cruises along the 64°W meridian between 25°N and 36°N, we have found that  $n\text{TCO}_2$  and  $n\text{TA}$  decrease southwards across the Sargasso Sea (Bates et al., 1996c). Thus the correlations between  $n\text{TCO}_2$ ,  $n\text{TA}$  and the SO index suggest that water masses passing through BATS change with time and that changes in the circulation patterns of the subtropical gyre contribute to the interplay between ocean biogeochemistry at BATS and climate variability.

These analyses indicate that NAO and ENSO play a role in modulating interannual hydrographic and biogeochemical variability at BATS. Local changes in vertical mixing, subtropical gyre circulation and mesoscale eddy frequency at BATS (as discussed in Section 4.6) are the likely oceanic responses to such atmospheric forcing. This statistical exercise, once again demonstrates the value of long time-series data sets in providing insight into large scale ocean variability. Linkages between climate variability and ocean biogeochemistry has implications for understanding other biogeochemical issues in the Sargasso Sea, including: the interaction between mixing, vertical nutrient supply and primary production; the impact of mesoscale eddies on biogeochemical cycling observed at BATS (e.g., McGillicuddy et al., 1999; Siegel et al., 1999); the carbon imbalance and oceanic DOC cycling (Michaels et al., 1994a; Carlson et al., 1994; Hansell and Carlson, 1998); variability in ecosystem community structure (e.g., Steinberg et al., 2001) and;

processes controlling nitrogen fixation in the Sargasso Sea (Michaels et al., 1996; Gruber et al., 1997; Orcutt et al., 2001). As BATS continues in the future, our understanding of how ocean biogeochemistry is influenced by climate variability will continue to improve.

## Acknowledgements

Anthony Knap, Anthony Michaels, Debbie Steinberg, Craig Carlson, and Dennis Hansell are thanked for their continued help and support. This research was supported by NOAA grant, and NSF grant OCE-9416565. My grateful thanks go to all the dedicated BATS technicians who have collected CO<sub>2</sub> samples over the years, including: Rod Johnson, Rachel Dow, Kjell Gundersen, Ann Close, Jens Sorensen, Melodie Hammer, Margaret Best, Frances Howse, Alice Doyle, Fred Bahr, Liz Caporelli, Tye Waterhouse, Susan Becker, Rhonda Kelly, Shannon Stone, Becky Little, Matthew Church, Peter Countway, Marta Sanderson, Kathy Rathburn, Karen Orcutt, Sarah Goldthwait, Steve Bell, Richard Owen, and Julian Mitchell. I thank Christine Pequignet for her help with cross-correlation analyses; the captains and crew of the R/V *Weatherbird II*, especially marine technicians Jeff Benson, Barry Bjork and James Caison; Andrew Dickson for CRM samples; Ken Johnson and Doug Wallace for loaning a D.O.E. sponsored SOMMA to BBSR; Taro Takahashi, Dave Chipman and John Goddard for their help with the *p*CO<sub>2</sub> system; Catherine Goyet for analysing the first two years of BATS TCO<sub>2</sub> samples and; Pieter Tans and Tom Conway for their atmospheric *x*CO<sub>2</sub> data. Craig Carlson, Dennis Hansell, Dave Siegel, Doug Wallace and 2 anonymous reviewers are thanked for their helpful comments.

## References

- Bates, N.R., Hansell, D.A., Carlson, C.A., Gordon, L.I., 1998a. Distribution of CO<sub>2</sub> species, estimates of net community production and air–sea CO<sub>2</sub> exchange in the Ross Sea polynya. *Journal of Geophysical Research* 103 (C2), 2883–2896.
- Bates, N.R., Knap, A.H., Bahr, F., Benson, J., Chipman, D.W., Howse, F., Johnson, R.J., Takahashi, T., 1998b. Carbon dioxide measurements obtained aboard the R/V *Weatherbird II* in the Sargasso Sea, June–December 1994. Bermuda Biological Station For Research Data Report, BBSR CO<sub>2</sub> Data Report 98-1, Ferry Reach, Bermuda.
- Bates, N.R., Knap, A.H., Bahr, F., Benson, J., Chipman, D.W., Howse, F., Johnson, R.J., Takahashi, T., 1998c. Carbon dioxide measurements obtained from the R/V *Weatherbird II* in the Sargasso Sea, January–December 1995. Bermuda Biological Station For Research Data Report, BBSR CO<sub>2</sub> Data Report 98-2, Ferry Reach, Bermuda.
- Bates, N.R., Knap, A.H., Michaels, A.F., 1998d. The effect of hurricanes on the local to global air–sea exchange of CO<sub>2</sub>. *Nature* 395, 58–61.
- Bates, N.R., Michaels, A.F., Knap, A.H., 1996a. Seasonal and interannual variability of the oceanic carbon dioxide system at the US JGOFS Bermuda Atlantic Time-series Site. *Deep-Sea Research II* 43 (2–3), 347–383.
- Bates, N.R., Michaels, A.F., Knap, A.H., 1996b. Alkalinity changes in the Sargasso Sea: geochemical evidence of calcification? *Marine Chemistry* 51, 347–358.
- Bates, N.R., Michaels, A.F., Knap, A.H., 1996c. Spatial variability of CO<sub>2</sub> species in the Sargasso Sea. *Caribbean Journal of Science* 32 (3), 262.
- Bates, N.R., Takahashi, T., Chipman, D.W., Knap, A.H., 1998e. Variability of *p*CO<sub>2</sub> on diel to seasonal timescales in the Sargasso Sea. *Journal of Geophysical Research* 103, 15 567–15 585.
- Bjerknes, J., 1964. Atlantic air–sea interaction. *Advances in Geophysics* 10, 1–82.

- Bojariu, R., 1997. Climate variability modes due to ocean–atmosphere interaction in the central Atlantic. *Tellus* 49A, 362–370.
- Brewer, P.G., 1978. Direct observation of the oceanic CO<sub>2</sub> increase. *Geophysical Research Letters* 5 (2), 997–1000.
- Brewer, P.G., Goldman, J., 1986. Alkalinity changes generated by phytoplankton growth. *Limnology and Oceanography* 21, 108–117.
- Brewer, P.G., Goyet, C., Friederich, G.E., 1997. Direct observation of the oceanic CO<sub>2</sub> increase revisited. *Proceedings of the National Academy of Sciences, USA* 94, 8308–8313.
- Butler, J.N., 1992. Alkalinity titration in seawater: how accurately can the data be fit by an equilibrium model? *Marine Chemistry* 38, 251–282.
- Carlson, C.A., Ducklow, H.W., Michaels, A.F., 1994. Annual flux of dissolved organic carbon from the euphotic zone in the northwestern Sargasso Sea. *Nature* 371, 405–408.
- Cayan, D.R., 1992a. Latent and sensible heat flux anomalies over the Northern Oceans: the connection to monthly atmospheric circulation. *Journal of Climate* 5, 354–369.
- Cayan, D.R., 1992b. Latent and sensible heat flux anomalies over the Northern Oceans: driving the sea surface temperature. *Journal of Physical Oceanography* 22, 859–881.
- Chatfield, C., 1989. *The Analysis of Time Series: An Introduction*. Chapman & Hall, London.
- Chen, C.-T.A., 1984. Oceanic penetration of excess CO<sub>2</sub> in a cross section between Alaska and Hawaii. *Geophysical Research Letters*, 117–119.
- Chen, C.-T.A., Millero, F.J., 1979. Gradual increase of oceanic CO<sub>2</sub>. *Nature* 277, 205–207.
- Curry, R.G., McCartney, M.S., Joyce, T.M., 1998. Oceanic transport of subpolar climate signals to mid-depth subtropical waters. *Nature* 391, 575–577.
- Davies, J.R., Rowell, D.P., Folland, C.K., 1997. North Atlantic and European seasonal predictability using an ensemble of multidecadal atmospheric GCM simulations. *International Journal of Climate* 17, 1263–1284.
- Dickson, R., Lazier, J., Meincke, J., Rhines, P., Swift, J., 1996. Long-term coordinated changes in the convective activity of the North Atlantic. *Progress in Oceanography* 38, 241–295.
- Dickson, R., Meincke, J., Malmberg, S.-A., Lee, A.J., 1988. The “Great Salinity Anomaly” in the northern North Atlantic 1968–1982. *Progress in Oceanography* 20, 103–151.
- Ebbesmeyer, C., Lindstrom, E.J., 1986. Structure and origin of 18°C water observed during the POLYMODE Local Dynamics Experiment. *Journal of Physical Oceanography* 16, 443–453.
- Enfield, D.B., Mayer, D.A., 1997. Tropical Atlantic sea surface temperature variability and its relation to El Niño–Southern Oscillation. *Journal of Geophysical Research* 102, 929–945.
- Enting, I.G., Trudinger, C.M., Francey, R.J., 1995. A synthetic inversion of the concentration and δ<sup>13</sup>C of atmospheric CO<sub>2</sub>. *Tellus* 47B, 35–52.
- Francey, R.J., Tans, P.P., Allison, C.E., Enting, I.G., White, J.W.C., Trolier, M., 1995. Changes in oceanic and terrestrial carbon uptake since 1982. *Nature* 373, 326–330.
- Goyet, C., Brewer, P.G., 1993. Biogeochemical properties of the oceanic carbon cycle. In: Willebrand, J., Anderson, D.L.T. (Eds.), *Modelling Oceanic Climate Interactions*. NATO ASI Series. I. Springer, Berlin.
- Goyet, C., Coatanoan, C., Eisheid, G., Amaoka, T., Okuda, K., Healy, R., Tsunogai, S., 1999. Spatial variation of total CO<sub>2</sub> and total alkalinity in the northern Indian Ocean: a novel approach for the quantification of anthropogenic CO<sub>2</sub> in seawater. *Journal of Marine Research* 57, 135–163.
- Goyet, C., Davis, D.L., 1997. Estimation of TCO<sub>2</sub> concentration throughout the water column. *Deep-Sea Research I* 44, 859–877.
- Goyet, C., Peltzer, E.T., 1994. Comparison of the August–September 1991 and 1979 surface partial pressure of CO<sub>2</sub> distribution in the Equatorial Pacific Ocean near 150°W. *Marine Chemistry* 45, 257–266.
- Gran, G., 1952. Determination of the equivalence point in potentiometric titrations. *Analyst* 77, 661–671.
- Gruber, N., Keeling, C.D., Stocker, T.F., 1998. Carbon-13 constraints on the seasonal inorganic carbon budget at the BATS site in the northwestern Sargasso Sea. *Deep-Sea Research I* 45, 673–717.
- Gruber, N., Sarmiento, 1997. Global patterns of marine nitrogen fixation and denitrification. *Global Biogeochemical Cycles* 11, 235–266.
- Gruber, N., Sarmiento, J.L., Stocker, T.F., 1996. An improved method for detecting anthropogenic CO<sub>2</sub> in the oceans. *Global Biogeochemical Cycles* 10, 809–837.

- Halliwell, G.R., Peng, G., Olson, D.B., 1994. Stability of the Sargasso Sea Subtropical Frontal Zone. *Journal of Physical Oceanography* 24, 1166–1183.
- Hansell, D.A., Carlson, C.A., 1998. Net community production of dissolved organic carbon. *Global Biogeochemical Cycles* 12, 443–453.
- Hazeleger, W., Drifhout, S.S., 1998. Mode water variability in a model of the subtropical gyre: response to atmospheric forcing. *Journal of Physical Oceanography* 28, 266–288.
- Hurrell, J.W., 1995. Decadal trends in the North Atlantic Oscillation: regional temperatures and precipitation. *Science* 269, 676–679.
- Hurrell, J.W., Van Loon, H., 1997. Decadal variations in climate associated with the North Atlantic Oscillation. *Climatic Change* 36, 301–326.
- Jenkins, W.J., 1982. On the climate of a subtropical gyre: decade timescale variations in water mass renewal in the Sargasso Sea. *Journal of Marine Research* 40 (supplement), 265–290.
- Johnson, K.M., King, A.E., Sieburth, J.McN., 1985. Coulometric  $\text{TCO}_2$  analyses for marine studies: an introduction. *Marine Chemistry* 16, 61–82.
- Johnson, K.M., Sieburth, J.McN., Williams, P.J.leB., Brandstrom, L., 1987. Coulometric total carbon dioxide analysis for marine studies: automation and calibration. *Marine Chemistry* 21, 117–133.
- Johnson, K.M., Wills, K.D., Butler, D.B., Johnson, W.K., Wong, C.S., 1993. Coulometric total carbon dioxide analysis for marine studies: maximizing the performance of an automated gas extraction system and coulometric detector. *Marine Chemistry* 44, 167–188.
- Jones, C.G., Thorncroft, C.D., 1998. The role of El Niño in Atlantic tropical cyclone activity. *Weather* 53, 324–336.
- Joyce, T.M., Robbins, P., 1996. The long-term hydrographic record at Bermuda. *Journal of Climate* 9, 3121–3131.
- Keeling, C.D., 1993. Surface ocean  $\text{CO}_2$ . In: Heimann, M. (Ed.), *Global Carbon Cycle*. Kluwer Academic Publishers, Dordrecht, pp. 22–29.
- Keeling, C.D., Bacastow, R.B., Carter, A.F., Piper, S.C., Whorf, T.P., Heimann, M., Mook, W.G., Roeloffzen, H., 1989. A three-dimensional model of atmospheric  $\text{CO}_2$  transport based on observed winds 1. Analysis of observational data. In: Peterson, D.H. (Ed.), *Aspects of Climate Variability the Pacific and the Western Americas*, Vol. 55. American Geophysical Union, *Geophysical Monograph*, pp. 165–236.
- Keeling, C.D., Whorf, T.P., Wahlen, M., Van der Plicht, J., 1995. Interannual extremes in the rate of rise of atmospheric carbon dioxide since 1980. *Nature* 375, 666–670.
- Keeling, R.F., Shertz, S.R., 1992. Seasonal and interannual variations in atmospheric oxygen and implications for the global carbon cycle. *Nature* 358, 723–727.
- Kapala, A., Maechel, H., Flohn, H., 1998. Behaviour of the centres of action above the Atlantic since 1881—Part II. Associations with regional climate anomalies. *International Journal of Climatology* 18, 23–36.
- Knap, A.H., Michaels, A.F., Dow, R.L., Johnson, R.J., Gundersen, K., Close, A., Howse, F., Bates, N.R., Hammer, M., Doyle, A., Waterhouse, T., Kelly, R., Becker, S., Little, B., 1995. US JGOFS Bermuda Atlantic Time-series Study. Data Report for BATS 49–BATS 60, October 1992–September 1993. US JGOFS Planning and Coordination Office, Woods Hole, MA.
- Knap, A.H., Michaels, A.F., Dow, R.L., Johnson, R.J., Gundersen, K., Knauer, G.A., Lohrenz, S.E., Asper, V.A., Tuel, M., Ducklow, H., Quinby, H., Brewer, P.G., 1991. US JGOFS Bermuda Atlantic Time-series Study Data Report 1 BATS 1–12, October 1988–September 1989. US JGOFS Planning and Coordination Office, Woods Hole, MA.
- Knap, A.H., Michaels, A.F., Dow, R.L., Johnson, R.J., Gundersen, K., Sorensen, J.C., Close, A., Howse, F., Hammer, M., Bates, N.R., Best, M., Doyle, A., Waterhouse, T., 1994. US JGOFS Bermuda Atlantic Time-series Study. Data Report for BATS 37–BATS 48, October 1991–September 1992. US JGOFS Planning and Coordination Office, Woods Hole, MA.
- Knap, A.H., Michaels, A.F., Dow, R.L., Johnson, R.J., Gundersen, K., Sorensen, J.C., Close, A., Howse, F., Hammer, M., Bates, N.R., Knauer, G.A., Lohrenz, S.E., Asper, V.A., Tuel, M., Ducklow, H., Quinby, H., 1993. US JGOFS Bermuda Atlantic Time-series Study. Data Report for BATS 25–BATS 36, October 1990–September 1991. US JGOFS Planning and Coordination Office, Woods Hole, MA.
- Knap, A.H., Michaels, A.F., Dow, R.L., Johnson, R.J., Gundersen, K., Sorensen, J., Close, A., Knauer, G.A., Lohrenz, S.E., Asper, V.A., Tuel, M., Ducklow, H., Quinby, H., Brewer, P.G., 1992. US JGOFS Bermuda Atlantic Time-series Study Data Report 2 BATS 13–24, October 1989–September 1990. US JGOFS Planning and Coordination Office, Woods Hole, MA.

- Knap, A.H., Michaels, A.F., Hansell, D.A., Bahr, F., Bates, N.R., Becker, S., Caporelli, E., Close, A.R., Doyle, A.P., Dow, R.L., Johnson, R.J., Kelly, R., Little, R., Gundersen, K., Howse, F.A., Waterhouse, T., 1997a. US JGOFS Bermuda Atlantic Time-series Study. Data Report for BATS 61–BATS 72, October 1993–September 1994. US JGOFS Planning and Coordination Office, Woods Hole, MA, 281pp.
- Knap, A.H., Michaels, A.F., Steinberg, D.K., Bahr, F., Bates, N.R., Bell, S., Countway, P., Close, A.R., Doyle, A.P., Dow, R.L., Howse, F.A., Gundersen, K., Johnson, R.J., Kelly, R., Little, R., Orcutt, K., Parsons, R., Rathburn, C., Sanderson, M., Stone, S., 1997b. BATS Methods Manual, Version 4, April 1997, US JGOFS Planning and Coordination Office, Woods Hole, MA, 136pp.
- Marchal, O., Monfray, P., Bates, N.R., 1996. Spring–summer imbalance in dissolved inorganic carbon in the mixed layer of the Northwestern Sargasso Sea. *Tellus* 48, 115–134.
- McGillicuddy, D.J., Johnson, R.J., Siegel, D.A., Michaels, A.F., Bates, N.R., Knap, A.H., 1999. Mesoscale variations of biogeochemical properties in the Sargasso Sea. *Journal of Geophysical Research* 104, 13 381–13 394.
- McGillicuddy, D.J., Robinson, A.R., 1997. Eddy induced nutrient supply and new production in the Sargasso Sea. *Deep-Sea Research I* 44, 1427–1449.
- McGillicuddy, D.J., Robinson, A.R., Siegel, D.A., Jannasch, H.W., Johnson, R., Dickey, T.D., McNeil, J., Michaels, A.F., Knap, A.H., 1998. Influence of mesoscale eddies on new production in the Sargasso Sea. *Nature* 394, 263–265.
- Menzel, D.W., Ryther, J.H., 1960. The annual cycle of primary production in the Sargasso Sea off Bermuda. *Deep-Sea Research* 6, 351–367.
- Menzel, D.W., Ryther, J.H., 1961. Annual variation in primary production of the Sargasso Sea off Bermuda. *Deep-Sea Research* 7, 282–288.
- Michaels, A.F., Bates, N.R., Buesseler, K.O., Carlson, C.A., Knap, A.H., 1994a. Carbon system imbalances in the Sargasso Sea. *Nature* 372, 537–540.
- Michaels, A.F., Knap, A.H., 1996. Overview of the US JGOFS Bermuda Atlantic Time-series Study and the Hydrostation S program. *Deep-Sea Research II* 43, 157–198.
- Michaels, A.F., Knap, A.H., Dow, R.L., Gundersen, K., Johnson, R.J., Sorensen, J., Close, A., Knauer, G.A., Lohrenz, S.E., Asper, V.A., Tuel, M., Bidigare, R.R., 1994b. Seasonal patterns of ocean biogeochemistry at the US JGOFS Bermuda Atlantic Time-series Study site. *Deep-Sea Research* 41, 1013–1038.
- Michaels, A.F., Olson, D., Sarmiento, J.L., Ammerman, J., Fanning, K., Jahnke, R., Knap, A.H., Lipshultz, F.J., Prospero, J., 1996. Inputs, losses and transformations of nitrogen and phosphorus in the deep North Atlantic Ocean. *Biogeochemistry* 35, 181–226.
- Millero, F.J., Lee, K., Roche, M., 1998. Distribution of alkalinity in the surface waters of the major oceans. *Marine Chemistry* 60, 111–130.
- Orcutt, K.M., Lipshultz, F., Gundersen, K., Arimoto, R., Michaels, A.F., Knap, A.H., Gallon, J.R., 2001. A seasonal study of the significance of N<sub>2</sub> fixation by *Trichodesmium* spp. at the Bermuda Atlantic Time-series Study (BATS) site. *Deep-Sea Research II* 48, 1583–1608.
- Penland, C., Matrosova, L., 1998. SST anomaly in the El Nino region is a strong 6 month predictor of SST anomaly in the north Tropical Atlantic. *Journal of Climate* 11, 483–490.
- Quay, P.D., Tilbrook, B., Wong, C.S., 1992. Oceanic uptake of fossil fuel CO<sub>2</sub>: carbon-13 evidence. *Science* 256, 74–79.
- Rodwell, M.J., Rowell, D.P., Folland, C.K., 1999. Oceanic forcing of the wintertime North Atlantic Oscillation and European climate. *Nature* 398, 320–323.
- Sarmiento, J.L., Murnane, R., Le Quéré, C., 1995. Air–sea CO<sub>2</sub> transfer and the carbon budget of the North Atlantic. *Philosophical Transactions of the Royal Society. B (London)* 348, 211–219.
- Sarmiento, J.L., Orr, J.C., Siegenthaler, U., 1992. A perturbation simulation of CO<sub>2</sub> uptake in an ocean general circulation model. *Journal of Geophysical Research* 97, 3621–3645.
- Shiller, A.M., 1981. Calculating the oceanic CO<sub>2</sub> increase: a need for caution. *Journal of Geophysical Research* 86, 11 083–11 088.
- Siegel, D.A., McGillicuddy, D.J., Fields, E.A., 1999. Mesoscale eddies, satellite altimetry and new production in the Sargasso Sea. *Journal of Geophysical Research* 104, 13 359–13 379.
- Sprintall, J., Tomczak, M., 1992. Evidence of the barrier layer in the surface layer of the tropics. *Journal of Geophysical Research* 97 (C5), 7305–7316.

- Steinberg, D.K., Carlson, C.A., Bates, N.R., Johnson, R.J., Michaels, A.F., Knap, A.H., 2001. Overview of the US JGOFS Bermuda Atlantic Time-series Study (BATS): a decade-scale look at ocean biology and biogeochemistry. *Deep-Sea Research II* 48, 1405–1447.
- Stocker, T.F., Broecker, W.S., Wright, D.G., 1994. Carbon uptake experiments with a zonally averaged global ocean circulation model. *Tellus* 46B, 103–122.
- Takahashi, T., Feely, R.A., Weiss, R.F., Wanninkhof, R., Chipman, D.W., Sutherland, S.C., Takahashi, T., 1997. Global air–sea flux of CO<sub>2</sub>: an estimate based on measurements of sea–air pCO<sub>2</sub> difference. *Proceedings of the National Academy of Science, USA*. 94, 8292–8299.
- Takahashi, T., Olafsson, J., Goddard, J.G., Chipman, D., Sutherland, S.C., 1993. Seasonal variation of CO<sub>2</sub> and nutrients in the high-latitude surface oceans: a comparative study. *Global Biogeochemical Cycles* 7 (4), 843–878.
- Talley, L., Raymer, M.E., 1982. Eighteen degree water variability. *Journal of Marine Research* 40, 757–775.
- Tans, P.P., Fung, I.Y., Takahashi, T., 1990. Observational constraints on the global atmospheric CO<sub>2</sub> budget. *Science* 247, 1431–1438.
- Taylor, A.H., Jordan, M.B., Stephens, J.A., 1998. Gulf Stream shifts following ENSO events. *Nature* 393, 638–640.
- Taylor, A.H., Stephens, J.A., 1998. The North Atlantic Oscillation and the latitude of the Gulf Stream. *Tellus* 50A, 134–142.
- Trenberth, K.E., 1984. Signal versus noise in the Southern Oscillation. *Monthly Weather Review* 112, 326–332.
- Trenberth, K.E., 1997. The Definition of El Niño. *Bulletin of the American Meteorological Society* 78, 2771–2777.
- Wallace, D.W.R., 1995. Monitoring global ocean carbon inventories. Ocean Observing System Development Panel, OOSDP Background Report No. 5, Texas A&M University, College Station, TX, 54pp.
- Winn, C.D., Li, Y.-H., Mackenzie, F.T., Karl, D.M., 1998. Rising surface ocean dissolved inorganic carbon at the Hawaii Ocean Time-series site. *Marine Chemistry* 60, 33–47.
- Winn, C.D., Mackenzie, F.T., Carillo, C.J., Sabine, C.L., Karl, D.M., 1994. Air–sea carbon dioxide exchange in the North Pacific subtropical gyre: implications for the global carbon budget. *Global Biogeochemical Cycles* 8 (2), 157–163.
- Worthington, L., 1976. On the North Atlantic Circulation. *The Johns Hopkins Oceanographic Studies*, 6, 110pp.
- Zhang, M.H., Cess, R.D., Xie, S.C., 1996. Relationship between cloud radiative forcing and sea surface temperatures over the entire tropical oceans. *Journal of Climate* 9, 1374–1384.